Inorganic Chemistry
Article

*Inorg. Chem.* **2009**, *48*, 8803–8810 **8803**
DOI: 10.1021/ic900981q

# Complex Formation and Molecular Structure of Neptunyl(VI) and -(V) Acetates

**Koichiro Takao,* Shinobu Takao, Andreas C. Scheinost, Gert Bernhard, and Christoph Hennig**

*Institute of Radiochemistry, Forschungszentrum Dresden-Rossendorf, P.O. Box 51 01 19, 01314 Dresden, Germany*

Received May 19, 2009

Stability and coordination of neptunyl(VI) and -(V) acetate complexes in aqueous solution were studied by using UV−vis−near-IR (NIR) and X-ray absorption fine structure (XAFS) spectroscopy. In the neptunyl(VI) acetate system, the formation of $Np^{VI}O_2(AcO)^+$, $Np^{VI}O_2(AcO)_2(aq)$, and $Np^{VI}O_2(AcO)_3^-$ was detected. Both spectroscopic methods provided similar stability constants: $\log K_1 = 2.98 \pm 0.01$, $\log \beta_2 = 4.60 \pm 0.01$, and $\log \beta_3 = 6.34 \pm 0.01$ from UV−vis−NIR and $\log K_1 = 2.87 \pm 0.03$, $\log \beta_2 = 4.20 \pm 0.06$, and $\log \beta_3 = 6.00 \pm 0.01$ from XAFS at $I = 0.30$ M $(H,NH_4)ClO_4$. Extended XAFS (EXAFS)-derived structural data for $Np^{VI}O_2^{2+}(aq)$, $Np^{VI}O_2(AcO)^+$, and $Np^{VI}O_2(AcO)_3^-$ were consistent with their stoichiometry, showing a bidentate coordination of acetate ($Np-O_{ax} = 1.76-1.77$ Å; $Np-O_{eq} = 2.43-2.47$ Å; $Np-C_c = 2.87$ Å; $Np-C_t = 4.38$ Å). Similar to $Np^{VI}$, $Np^V$ forms also three different complexes with acetate. The stability constants of $Np^VO_2(AcO)(aq)$, $Np^VO_2(AcO)_2^-$, and $Np^VO_2(AcO)_3^{2-}$ were determined by UV−vis−NIR titration to $\log K_1 = 1.93 \pm 0.01$, $\log \beta_2 = 3.11 \pm 0.01$, and $\log \beta_3 = 3.56 \pm 0.01$ at $I = 0.30$ M $(H,NH_4)ClO_4$. The present result is corroborated by the structural information from EXAFS ($Np-O_{ax} = 1.83-1.85$ Å; $Np-O_{eq} = 2.51$ Å; $Np-C_c = 2.90-2.93$ Å) and by the electrochemical behavior of the $Np^{V/VI}$ redox couple in the presence of AcOH as a function of the pH.

## 1. Introduction

Thermodynamics is important to describe the species distribution of a metal ion ($M^{n+}$) under specific conditions. Several methods are available to determine equilibrium constants of complexes, including potentiometry and spectrophotometry.[1,2] Recently, UV−vis−near-IR (NIR) absorption spectrophotometry became attractive because of the combination with statistical data treatment. This technique provides information on complexation reactions based on spectral changes as functions of pH, ligand concentration, temperature, stoichiometry of complexes, and stability constants. However, one cannot derive the exact structural details of involved species from the UV−vis−NIR absorption spectrum. This gap can be filled by using other spectroscopic techniques that are sensitive to the chemical bonds, e.g., X-ray absorption fine structure (XAFS) spectroscopy. The extended XAFS (EXAFS) spectrum provides one-dimensional information on the coordination sphere around a target atom of interest, such as the coordination numbers ($N$) of the surrounding atoms and their distances ($R$) to the central atom $M^{n+}$.[3] These structural parameters are necessary to generate reliable thermodynamic equations.

Solution chemistry of actinides is an important issue in nuclear engineering, especially for nuclear fuel reprocessing and risk assessments of radionuclide migration in the geosphere.[4,5] Carboxylates comprise a group of typical organic ligands occurring in natural environments, forming strong complexes with actinides. Acetate ($AcO^-$) is a simple monocarboxylate and is frequently used as a model species to simulate the complexation behavior of more complicated ligands such as humic acid. Only a limited number of studies are available on the complexation of neptunyl(VI) and -(V)

*To whom correspondence should be addressed. E-mail: k.takao@fzd.de. Phone: +49 351 260-2076.

(1) Cookson, R. F. *Chem. Rev.* **1974**, *74*, 5–28.

(2) (a) Grenthe, I., Fuger, J., Konings, R. J. M., Lemire, R. J., Muller, A. B., Nguyen-Trung, C., Wanner, H., Forest, I., Eds. (NEA-OECD). *Chemical Thermodynamics of Uranium*; North-Holland−Elsevier Science Publishers BV: Amsterdam, The Netherlands, 1992; Vol. *1*. (b) Fuger, J.; Spahiu, K.; Nitsche, H.; Sullivan, J. C.; Ullman, W. J.; Potter, P.; Vitorge, P.; Rand, M. H.; Wanner, H.; Rydberg, J. *Chemical Thermodynamics of Neptunium and Plutonium*; Elsevier Science BV: Amsterdam, The Netherlands, 2001. (c) Fanghänel, T.; Neck, V.; Fuger, J.; Palmer, D. A.; Grenthe, I.; Rand, M. H. *Update on the Chemical Thermodynamics of Uranium, Neptunium, Plutonium, Americium and Technetium*; Elsevier Science BV: Amsterdam, The Netherlands, 2003.

(3) (a) Denecke, M. A. *Coord. Chem. Rev.* **2006**, *250*, 730–754. (b) Clark, D. L.; Conradson, S. D.; Ekberg, S. A.; Hess, N. J.; Neu, M. P.; Palmer, P. D.; Runde, W.; Drew Tait, C. *J. Am. Chem. Soc.* **1996**, *118*, 2089–2090. (c) Docrat, T. I.; Mosselmans, J. F. W.; Charnock, J. M.; Whiteley, M. W.; Collison, D.; Livens, F. R.; Jones, C.; Edmiston, M. J. *Inorg. Chem.* **1999**, *38*, 1879–1882. (d) Bolvin, H.; Wahlgren, U.; Moll, H.; Reich, T.; Geipel, G.; Fanghänel, T.; Grenthe, I. *J. Phys. Chem. A* **2001**, *105*, 11441–11445. (e) Ikeda, A.; Hennig, C.; Tsushima, S.; Takao, K.; Ikeda, Y.; Scheinost, A. C.; Bernhard, G. *Inorg. Chem.* **2007**, *46*, 4212–4219. (f) Ikeda, A.; Hennig, C.; Rossberg, A.; Tsushima, S.; Scheinost, A. C.; Bernhard, G. *Anal. Chem.* **2008**, *80*, 1102–1110. (g) Ikeda-Ohno, A.; Hennig, C.; Rossberg, A.; Funke, H.; Scheinost, A. C.; Bernhard, G.; Yaita, T. *Inorg. Chem.* **2008**, *47*, 8249–8305.

(4) Kaszuba, J. P.; Runde, W. H. *Environ. Sci. Technol.* **1999**, *33*, 4427–4433.

(5) Icopini, G. A.; Boukhalfa, H.; Neu, M. P. *Environ. Sci. Technol.* **2007**, *41*, 2764–2769.

© 2009 American Chemical Society
Published on Web 08/19/2009

by acetate and its derivatives in aqueous solutions.[6−8] These studies suggest for $Np^{VI}$ a complex stoichiometry of $Np^{VI}O_2(AcO)_n^{2-n}$ with $n = 1-3$. In contrast, for $Np^{V}$, only one complex, $Np^{V}O_2(AcO)(aq)$, was reported, with its stability constants widely scattered among different reports.[7] The solid neptunyl(V) and -(VI) acetates and related complexes (e.g., propionate, phthalate, oxalate) were extensively investigated by using single-crystal and powder X-ray diffraction methods.[9−13] These studies provide structures for $Np^{VI}O_2(AcO)_3^-$ and $Np^{V}O_2(AcO)_3^{2-}$ isolated as $Na^+$ and $Ba^{2+}$ salts, respectively.[9a,10a] The solid $BaNp^{V}O_2(AcO)_3$ suggests that a tris(acetato)neptunyl(V) complex is likely to be present in solution, related to the stepwise complexation reactions of $Np^{V}O_2(AcO)_n^{1-n}$ with $n = 1-3$. Additionally, $Np^{V}$ may form various polynuclear species, where several $Np^{V}O_2^+$ ions interact through the axial oxygen (i.e., cation−cation interaction)[13,14] or through bridging ligands such as oxalate.[11] This property makes the interpretation of $Np^{V}$ solution chemistry with carboxylates including acetate more complicated.

This unsatisfying situation motivated us to combine EXAFS and UV−vis−NIR spectroscopy to investigate the complexation reactions of neptunyl(VI) and -(V) with acetate in aqueous solution. Our aim is to provide the proper reaction schemes by combining thermodynamic parameters and structural information.

## 2. Experimental Section

***Caution!*** *Neptunium-237 is a radioactive isotope ($T_{1/2} = 2.14 \times 10^6$ years) and an α-emitter. It has to be handled in dedicated facilities with appropriate equipment for radioactive materials to avoid health risks caused by radiation exposure. Perchloric acid and its salts are potentially explosive. Handling of all compounds containing $ClO_4^-$ should be done with great care and in small amounts. The heating process of neptunium with $HClO_4$ is most hazardous. Any contacts with organic materials should be avoided.*

**Sample Preparation.** Neptunium-237 from CEA-Marcoule (France) was purified through precipitation by alkalization and column chromatography with an anion-exchange resin (Dowex 1X8) in $HNO_3$(aq). The recovered neptunium was oxidized to 6+ by heating with $HNO_3$ until dry. The residue was dissolved in 1.0 M $HClO_4$. This solution was heated again to dryness. To expel $HNO_3$ and excess $HClO_4$ from $NpO_2(ClO_4)_2 \cdot nH_2O$, cycles of adding small volumes of water and heating to dryness were repeated until no white fume was observed and no acid was detected in the vapor by pH test paper. The residual $NpO_2(ClO_4)_2 \cdot nH_2O$ was dissolved in 1.0 M $HClO_4$. This solution was used as a stock solution of $Np^{VI}$. Sample solutions for UV−vis−NIR and XAFS spectroscopy were prepared by mixing a portion of the $Np^{VI}$ stock solution with glacial acetic acid (AcOH, Merck) and 70 wt % $HClO_4$ (Merck). The concentrations of total $Np^{VI}$ in the samples were determined spectrophotometrically ($2.93 \times 10^{-3}$ M for UV−vis−NIR and $1.36 \times 10^{-2}$ M for XAFS) by using molar absorptivity data from the literature.[15,16] In all $Np^{VI}$ samples, the total concentration of acetate was kept at 1.00 M. The pH value of each sample was adjusted by adding 25 wt % $NH_3$(aq) (Merck). The ionic strength ($I$) was fixed to 0.30 M $(H,NH_4)ClO_4$ by conversion of $H^+$ to $NH_4^+$ with pH variation.

A sample solution of $Np^{V}$ was prepared by the electrochemical reduction of $Np^{VI}$ in 1.00 M AcOH + 0.30 M $HClO_4$(aq) at 0.50 V vs Ag/AgCl. Completion of the electrolysis was confirmed spectrophotometrically. The concentrations of total $Np^{VI}$ in the samples were determined spectrophotometrically ($2.78 \times 10^{-3}$ M for UV−vis−NIR and $2.00 \times 10^{-2}$ M for XAFS).[15,16] In all $Np^{V}$ samples, the total concentration of acetate was kept at 1.00 M, and $I$ was fixed to 0.30 M $(H,NH_4)ClO_4$.

**Methods.** UV−vis−NIR absorption spectra of the $Np^{VI}$ and $Np^{V}$ series were recorded by a Varian Cary 5G spectrophotometer. The light intensity every 0.2 nm was integrated for 0.1 s with a 2.0 nm slit width and recorded as absorbance. All measurements were carried out at 295 ± 1 K.

XAFS experiments were performed at the Rossendorf Beamline (BM20) at the European Synchrotron Radiation Facility (6 GeV, 60−80 mA).[17] An Si(111) double-crystal monochromator was employed in channel-cut mode to monochromatize white X-ray light from the synchrotron. Np $L_{III}$-edge XAFS spectra of the $Np^{VI}$ and $Np^{V}$ samples with AcOH were recorded in transmission mode by using argon-filled ionization chambers at ambient temperature (295 ± 1 K) and pressure. The X-ray energy in each experimental run was calibrated by a Y foil placed after the sample (first inflection point at 17 038 eV). The XAFS spectrum of each sample was accumulated twice and merged.

(6) (a) Mefod'eva, M. P.; Artyukhin, P. I.; Gel'man, A. D. *Radiokhimiya* **1959**, *1*, 309. (b) Portanova, R.; Tomat, G.; Magon, L.; Cassol, A. *J. Inorg. Nucl. Chem.* **1970**, *32*, 2343–2348.

(7) (a) Rösch, F.; Dittrich, S.; Buklanov, G. V.; Milanov, M.; Khalkin, V. A.; Dreyer, R. *Radiochim. Acta* **1990**, *49*, 29–34. (b) Rizkalla, F. N.; Nectoux, F.; Dabos-Seignon, S.; Pagés, M. *Radiochim. Acta* **1990**, *51*, 113–117. (c) Novak, C. F.; Borkowski, M.; Choppin, G. R. *Radiochim. Acta* **1996**, *74*, 111–116. (d) Borkowski, M.; Lis, S.; Choppin, G. R. *Radiochim. Acta* **1996**, *74*, 117–121. (e) Pokorvsky, O. S.; Choppin, G. R. *Radiochim. Acta* **1997**, *79*, 167−171 and references cited therein.

(8) For example, see:(a) Gruen, D. M.; Katz, J. J. *J. Am. Chem. Soc.* **1953**, *75*, 3772–3776. (b) Nash, K.; Fried, S.; Friedman, A. M.; Sullivan, J. C. *Environ. Sci. Technol.* **1981**, *15*, 834–837. (c) Bessonov, A. A.; Krot, N. N.; Grigor'ev, M. S. *Radiokhimiya* **2006**, *48*, 123–127. (d) Shcherbina, N. S.; Perminova, I. V.; Kalmykov, S. N.; Haire, R. G.; Novikov, A. P. *Environ. Sci. Technol.* **2007**, *79*, 167–171.

(9) (a) Alcock, N. W.; Roberts, M. M. *J. Chem. Soc., Dalton Trans.* **1982**, 33–36. (b) Charushnikova, I. A.; Krot, N. N.; Polyakova, I. N.; Starikova, Z. A. *Radiokhimiya* **2007**, *49*, 106–110.

(10) (a) Burns, J. H.; Musikas, C. *Inorg. Chem.* **1977**, *16*, 1619–1622. (b) Andreev, G. B.; Budantseva, N. A.; Tananaev, I. G.; Myasoedov, B. F. *Inorg. Chem.* **2008**, *47*, 2943–2945. (c) Andreev, G. B.; Budantseva, N. A.; Tananaev, I. G.; Myasoedov, B. F. *Inorg. Chem.* **2009**, *48*, 1232–1235.

(11) (a) Grigor'ev, M. S.; Charushnikova, I. A.; Starikova, Z. A.; Krot, N. N.; Polyakova, I. N. *Radiokhimiya* **2004**, *46*, 212–215. (b) Charushnikova, I. A.; Krot, N. N.; Polyakova, I. N. *Radiokhimiya* **2005**, *47*, 495–499. (c) Charushnikova, I. A.; Krot, N. N.; Polyakova, I. N. *Radiokhimiya* **2006**, *48*, 3–6. (d) Charushnikova, I. A.; Krot, N. N.; Polyakova, I. N. *Radiokhimiya* **2007**, *49*, 102–105. (e) Charushnikova, I. A.; Krot, N. N.; Starikova, Z. A.; Dolgushin, F. M.; Polyakova, I. N. *Radiokhimiya* **2008**, *50*, 31–33.

(12) (a) Bessonov, A. A.; Grigor'ev, M. S.; Afonas'eva, T. V.; Krot, N. N. *Radiokhimiya* **1989**, *31*, 33–37. (b) Charushnikova, I. A.; Afonas'eva, T. V.; Krot, N. N. *Radiokhimiya* **1995**, *37*, 9–14. (c) Nakada, M.; Yamashita, T.; Nakamoto, T.; Saeki, M.; Krot, N. N.; Grigor'ev, M. S. *Radiokhimiya* **2002**, *44*, 97–101. (d) Krot, N. N.; Bessonov, A. A.; Grigor'ev, M. S.; Charushnikova, I. A.; Makarenkov, V. I. *Radiokhimiya* **2004**, *46*, 389–395. (e) Bessonov, A. A.; Krot, N. N.; Charushnikova, I. A.; Makarenkov, V. I. *Radiokhimiya* **2007**, *49*, 197–201. (f) Bessonov, A. A.; Krot, N. N.; Grigor'ev, M. S.; Makarenkov, V. I. *Radiokhimiya* **2008**, *50*, 27–30.

(13) (a) Grigor'ev, M. S.; Yanovskii, A. I.; Struchkov, Y. T.; Bessonov, A. A.; Afonas'eva, T. V.; Krot, N. N. *Sov. Radiochem.* **1989**, *31*, 397–403. (b) Charushnikova, I. A.; Perminov, V. P.; Katser, S. B. *Radiokhimiya* **1995**, *37*, 493–498. (c) Grigor'ev, M. S.; Antipin, M. Y.; Krot, N. N. *Radiokhimiya* **2006**, *48*, 7–10.

(14) (a) Guillaume, B.; Hahn, R. L.; Narten, A. H. *Inorg. Chem.* **1983**, *22*, 109–111. (b) Skanthakumar, S.; Antonio, M. R.; Soderholm, L. *Inorg. Chem.* **2008**, *47*, 4591–4595. (c) Natrajan, L.; Burdet, F.; Pecaut, J.; Mazzanti, M. *J. Am. Chem. Soc.* **2006**, *128*, 7152–7153. (d) Burdet, F.; Pecaut, J.; Mazzanti, M. *J. Am. Chem. Soc.* **2006**, *128*, 16512–16513. (e) Nocton, G.; Horeglad, P.; Pecaut, J.; Mazzanti, M. *J. Am. Chem. Soc.* **2008**, *130*, 16633–16645.

(15) Katz, J. J.; Seaborg, G. T.; Morss, L. R. *The Chemistry of the Actinide Elements*, 2nd ed.; Chapman and Hall: London, 1986.

(16) (a) Sjoblom, R.; Hindman, J. C. *J. Am. Chem. Soc.* **1951**, *73*, 1744–1751. (b) Waggener, W. C. *J. Phys. Chem.* **1958**, *62*, 382–383. (c) Matsika, S.; Pitzer, R. M. *J. Phys. Chem. A* **2000**, *104*, 4064–4068. (d) Matsika, S.; Pitzer, R. M.; Reed, D. T. *J. Phys. Chem. A* **2000**, *104*, 11983–11992.

(17) Reich, T.; Bernhard, G.; Geipel, G.; Funke, H.; Hennig, C.; Rossberg, A.; Matz, W.; Schell, N.; Nitsche, H. *Radiochim. Acta* **2000**, *88*, 633–637.

**Chart 1**

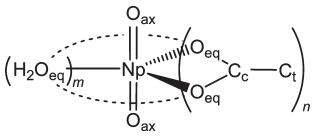


Cyclic voltammograms (CVs) of $5.0 \times 10^{-3}$ M $Np^{VI}$ with 1.00 M AcOH at $I = 0.30$ M $(H,NH_4)ClO_4$ and different pHs were recorded at $295 \pm 1$ K under a nitrogen gas atmosphere with an Autolab PGSTAT302 potentiostat/galvanostat (Eco Chemie BV). The three-electrode system consisted of a platinum disk working electrode (surface area: 2.0 $mm^2$), a platinum wire counter electrode, and an Ag/AgCl (3 M NaCl) reference electrode. To expel dissolved oxygen, nitrogen gas was passed through the samples at least 10 min prior to starting CV measurements.

**Data Treatment.** In order to calculate the stability constants, molar absorbance spectra of individual species, and speciation diagrams, the data sets of UV−vis−NIR and XAFS spectra at different pHs were analyzed using the nonlinear least-squares regression program *pHab2003*.[18] The logarithmic protonation constant of acetate (log $K_{AcO}$) was fixed at 4.45 at $I =$ v 0.3 M, which was estimated from log $K°_{AcO} = 4.757$ at $I = 0$[19] by correcting for the ionic strength.[2c] The obtained XAFS spectrum of the neptunyl(VI) acetate system at each pH was normalized by using the AUTOBK algorithm.[20]

EXAFS data extraction and fits were processed with IFEFFIT.[21] The threshold energy $E_0$ of Np $L_{III}$-edge was defined at 17 625 eV, regardless of the neptunium oxidation states. The curve fit was performed with Fourier-transformed spectra, i.e., in $R$ space, using phases and amplitudes calculated by *FEFF8.20*[22] based on the crystal structure of $NaNp^{VI}O_2(AcO)_3$.[9a] Single-scattering (SS) paths from coordinating axial and equatorial oxygen atoms ($O_{ax}$ and $O_{eq}$) and carboxylic and terminal carbon atoms in acetate ($C_c$ and $C_t$, if possible) and multiple-scattering (MS) paths from $O_{ax}-Np-O_{ax}$ and $Np-C_c-C_t$ were included in the EXAFS curve fit (Chart 1). The amplitude reduction factor $S_0^2$ was fixed to 0.9, and the shifts in the threshold energy $\Delta E_0$ were constrained to be the same value for all shells.

## 3. Results and Discussion

**3.1. Stability Constants and Structures of Neptunyl(VI) Acetate Complexes.** UV−vis−NIR absorption spectra of $Np^{VI}$ ($2.93 \times 10^{-3}$ M) with 1.00 M AcOH at $I =$ 0.30 M $(H,NH_4)ClO_4$ and different pHs are shown in Figure 1. All spectra are also displayed in Figure S1 of the Supporting Information. The spectra show the characteristic features of $Np^{VI}$, i.e., absorption bands at 450−800 nm and around 1200 nm attributable to f−f transitions of the $5f^1$ configuration.[15,16] With increasing pH, systematic spectral changes were observed. However, no isosbestic points were detected in this series. The absorbance around 500 and 560 nm increases from pH 0.50 to 2.78 and then decreases from pH 2.95 to 4.27. These observations indicate that several equilibria occur in this series. Because hydrolysis of $Np^{VI}$ is not significant in the applied pH range,[2b,c] the observed spectral change suggests a multistep complexation of neptunyl(VI) with acetate. In this sample series, a residual of $Np^V$ (< 3 mol % of total neptunium) was shown by the characteristic intense absorption band at 980 nm with $\varepsilon = 395\ M^{-1}\ cm^{-1}$.[15] Because there are no other intense absorption bands of $Np^V$, such a minor residual is unlikely to affect the following analysis. The stability constants of neptunyl(VI) acetate complexes were calculated from the pH dependence of the UV−vis−NIR spectra in Figure 1 by using *pHab2003*. To suppress the minor $Np^V$ and to eliminate the unnecessary load of computation for the spectroscopically silent region of $Np^{VI}$, the data points in the ranges of 610−625, 800−1000, and 1080−1120 nm[15] were omitted. Equivalently to the previously reported thermodynamic parameters,[6] the stability constants of neptunyl(VI) acetate complexes are determined according to the following equations.

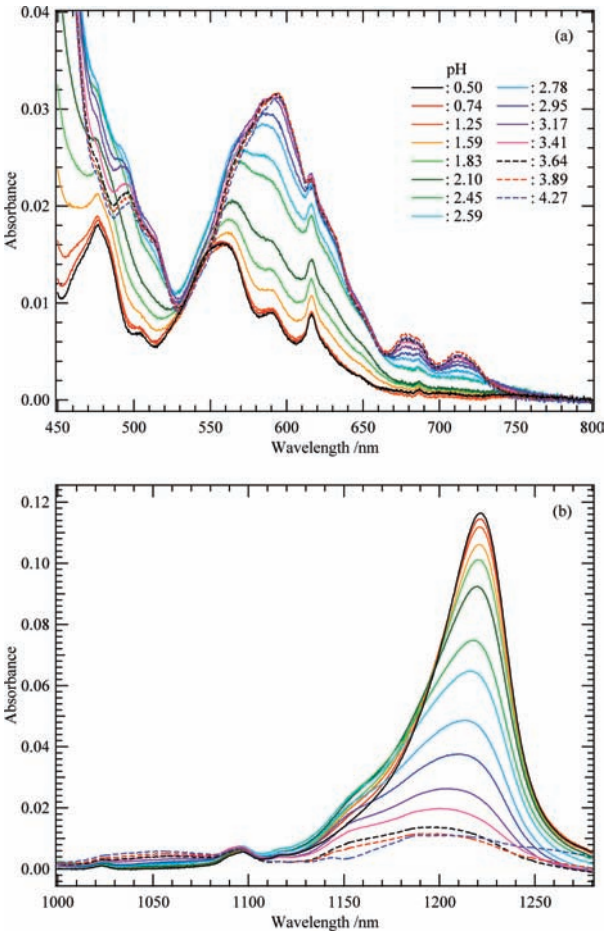


**Figure 1.** UV−vis−NIR absorption spectra of $Np^{VI}$ ($2.93 \times 10^{-3}$ M) with 1.00 M AcOH at $I = 0.30$ M $(H,NH_4)ClO_4$ and different pHs (0.50−4.27).

$$Np^{VI}O_2^{2+} + AcO^- = Np^{VI}O_2(AcO)^+ \quad (1)$$

$$Np^{VI}O_2^{2+} + 2AcO^- = Np^{VI}O_2(AcO)_2(aq) \quad (2)$$

$$Np^{VI}O_2^{2+} + 3AcO^- = Np^{VI}O_2(AcO)_3^- \quad (3)$$

The resulting stability constants are listed in Table 1 together with those reported in the literature, which were obtained by potentiometric titration. The obtained

(18) Gans, P.; Sabatini, A.; Vacca, A. *Ann. Chim.* **1999**, *89*, 45–49.
(19) Martell, A. E.; Smith, R. M. NIST Critically Selected Stability Constants of Metal Complexes; *NIST Standard Reference Database 46*, version 8.0; developed by Motekaitis, R. J.; distributed by NIST Standard Reference Data, **2004**.
(20) Newville, M.; Lvinš, P. *Phys. Rev. B* **1993**, *47*, 14126–14131.
(21) Ravel, B.; Newville, M. *J. Synchrotron Radiat.* **2005**, *12*, 537–541.
(22) Ankudinov, A. L.; Ravel, B.; Rehr, J. J.; Conradson, S. D. *Phys. Rev. B* **1998**, *58*, 7565–7576.

**Table 1.** Overall Stability Constants of Actinyl Acetate Complexes

| | $\log K_1$ | $\log \beta_2$ | $\log \beta_3$ | $I$/M | $T$/K | method | ref |
|---|---|---|---|---|---|---|---|
| $Np^{VI}$ | 2.98 ± 0.01 | 4.60 ± 0.01 | 6.34 ± 0.01 | 0.30 | 295 | UV−vis−NIR | this work |
| | 2.87 ± 0.03 | 4.20 ± 0.06 | 6.00 ± 0.01 | 0.30 | 295 | XAFS | this work |
| | 2.31 ± 0.02 | 4.23 ± 0.05 | 6.00 ± 0.03 | 1.0 | 293 | pot | 6b and 19 |
| $U^{VI}$ | 2.58 ± 0.03 | 4.37 ± 0.14 | 6.86 ± 0.04 | 1.05 | 298 | pot | 23 |
| | 2.43 ± 0.03 | 4.43 ± 0.06 | 6.45 ± 0.07 | 1.0 | 298 | | 19 |
| $Pu^{VI}$ | 2.13 | 3.49 | 5.01 | 1.0 | 298 | | 19 |
| $Np^{V}$ | 1.93 ± 0.01 | 3.11 ± 0.01 | 3.56 ± 0.01 | 0.30 | 295 | UV−vis−NIR | this work |

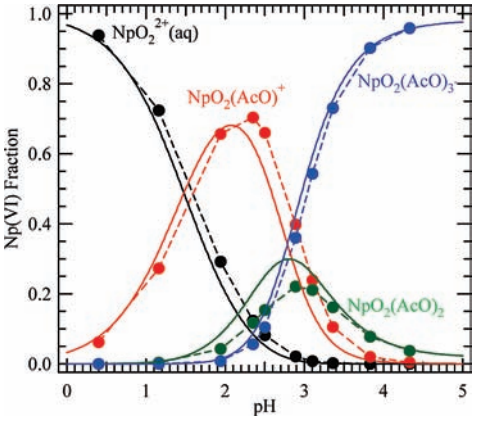


**Figure 2.** Species distribution of neptunyl(VI) acetates derived from UV−vis−NIR (solid lines) and XAFS (solid circles with dashed lines) spectroscopy at 0.015 M $Np^{VI}$ and 1 M AcOH in $I$ = 0.3 M.

stability constants are similar to the values from the literature.[6b,19] Absorption spectra of the extracted individual $Np^{VI}O_2(AcO)_n^{2-n}$ ($n$ = 0−3) complexes are displayed in Figure S2 of the Supporting Information. Furthermore, the stability constants of neptunyl(VI) acetates are in line with those of uranyl(VI)[19,23] and plutonyl(VI) acetates.[19] Using the stability constants of eqs 1−3 determined here, the species distribution of 15 mM $Np^{VI}$ in 1 M AcOH at $I$ = 0.3 M was calculated as shown in Figure 2 (smooth curves).

In the next step, Np $L_{III}$-edge XAFS of $Np^{VI}$ ($1.36 \times 10^{-2}$ M) with 1.00 M AcOH at $I$ = 0.30 M $(H,NH_4)ClO_4$ at various pHs was studied. The recorded XAFS spectra in normalized $\mu_0(E)$ are shown in Figure S3 (Supporting Information). Systematic changes with pH variation were observed in both XANES and EXAFS regions, indicating the structural modification around neptunyl(VI) due to complexation with acetate. This feature was also observed in the Fourier transforms (FTs; Figure S4 in the Supporting Information) of $k^3$-weighted EXAFS spectra from Figure S3 in the Supporting Information. Through eqs 1−3, the coordination of acetate is detectable as a peak due to its carbonyl carbon $C_c$. As shown in Figure S4 in the Supporting Information, the peak intensity of the Np−$C_c$ shell increases with increasing pH, being more clearly observed in the FT imaginary part.

The stability constants of the neptunyl(VI) acetate complexes were also calculated from the pH series of XAFS (normalized $\mu_0(E)$; Figure S3 in the Supporting Information) by using *pHab2003*. The obtained stability constants, shown in Table 1, are consistent with those obtained from the UV−vis−NIR spectra. Figure 2 also shows the species distribution calculated by using the formation constants from XAFS. The comparison demonstrates a good agreement between the formation constants obtained from UV−vis−NIR and EXAFS spectra. The extracted XANES and $k^3$-weighted EXAFS spectra of individual $Np^{VI}O_2(AcO)_n^{2-n}$ ($n$ = 0−3) species are shown in Figure S5 in the Supporting Information. Note that noise in the spectrum of $Np^{VI}O_2(AcO)_2$(aq) is high at $k > 10$ Å$^{-1}$ because this species is a minor component. Therefore, the structure parameters of $Np^{VI}O_2(AcO)_2$(aq) could not be determined properly and are not compared to those of other $NpO_2(AcO)_n^{2-n}$ species in the later discussion.

The $k^3$-weighted EXAFS spectra and FTs of $Np^{VI}O_2(AcO)_n^{2-n}$ ($n$ = 0, 1, 3) are shown in Figure 3 together with the best curve fits. The structural parameters of these neptunyl(VI) acetate species are summarized in Table 2. The intense FT peak around $R + \Delta = 1.34$ Å is assigned to the axial oxygen atoms ($O_{ax}$) representative of $NpO_2^{2+}$. For all three $Np^{VI}O_2(AcO)_n^{2-n}$ ($n$ = 0, 1, 3) complexes,

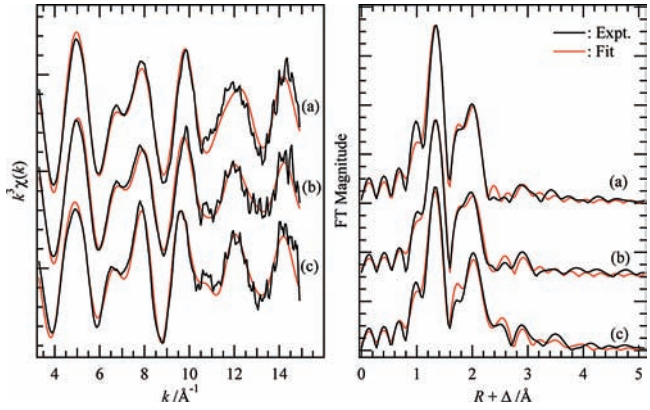


**Figure 3.** $k^3$-weighted Np $L_{III}$-edge EXAFS spectra (left) and their FTs (right) of individual $Np^{VI}$ species: $Np^{VI}O_2^{2+}$(aq) (a), $Np^{VI}O_2(AcO)^+$ (b), $Np^{VI}O_2(AcO)_3^-$ (c).

**Table 2.** Structural Parameters from EXAFS Curve Fits for Individual $Np^{VI}$ Species[a]

| | $Np^{VI}O_2^{2+}$(aq) | | | $Np^{VI}O_2(AcO)^+$ | | | $Np^{VI}O_2(AcO)_3^-$ | | |
|---|---|---|---|---|---|---|---|---|---|
| shell | $N$ | $R$/Å | $\sigma^2$/Å$^2$ | $N$ | $R$/Å | $\sigma^2$/Å$^2$ | $N$ | $R$/Å | $\sigma^2$/Å$^2$ |
| $O_{ax}$ | 2 [b] | 1.76 | 0.0020 | 2 [b] | 1.77 | 0.0027 | 2 [b] | 1.77 | 0.0023 |
| $O_{eq}$ | 4.5 | 2.43 | 0.0059 | 4.7 | 2.44 | 0.0073 | 5.4 | 2.47 | 0.0070 |
| $C_c$ | | | | 1.2 | 2.87 | 0.0010 | 2.7 | 2.87 | 0.0024 |
| $C_t$ | | | | | | | 2.7 [c] | 4.38 | 0.0100 |
| $O_{ax}$ (MS) | 2 [b] | 3.52 | 0.0040 | 2 [b] | 3.56 | 0.0030 | 2 [b] | 3.55 | 0.0030 |
| $C_t$ (MS) | | | | | | | 2.7 [c] | 4.38 | 0.0122 |
| | $\Delta E_0$ = 7.5 eV | | | $\Delta E_0$ = 11.4 eV | | | $\Delta E_0$ = 8.9 eV | | |

[a] $\sigma^2$ = Debye−Waller factor. [b] Fixed parameter. [c] Constrained at the same value as that of the $C_c$ shell.

(23) Jiang, J.; Rao, L.; Di Bernardo, P.; Zanonato, P. L.; Bismondo, A. *J. Chem. Soc., Dalton Trans.* **2002**, 1832–1838.

**Scheme 1.** Structures of $NpO_2^{2+}$ Complexes with Acetate

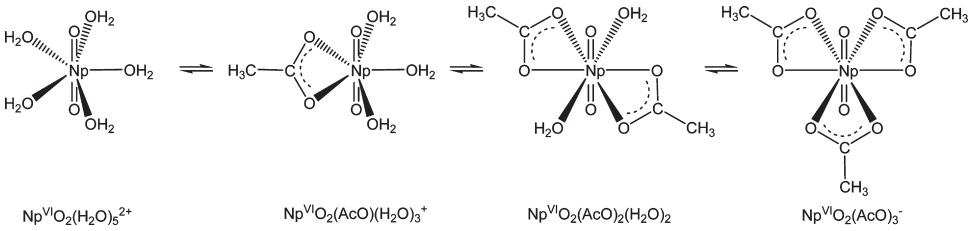


the Np−$O_{ax}$ distance remains constant at 1.76−1.77 Å. The peak around $R + \Delta = 2.0$ Å arises from the equatorial oxygen atoms ($O_{eq}$) of the coordinated $H_2O$ and/or acetate. Because the differences in the Np−$O_{eq}$ distances of $Np^{VI}O_2^{2+}$(aq) ($R = 2.44$ Å) and $Np^{VI}O_2(AcO)_3^-$ ($R = 2.47$ Å) binary complexes are too small to be resolved by EXAFS, the Np−$O_{eq}$ peak of the $Np^{VI}O_2(AcO)^+$ ternary complex (i.e., $Np^{VI}O_2^{2+}$-$AcO^-$-$H_2O$) was fit with an average Np−$O_{eq}$ distance of 2.44 Å, i.e., between that of $H_2O$ and acetate ligands. All Np−$O_{eq}$ distances determined here are similar to those of solid $U^{VI}O_2(H_2O)_5(ClO_4)_2$ (mean = 2.42 Å),[24] $NaNp^{VI}O_2(AcO)_3$ (mean = 2.46 Å),[9a] and $NaNp^{VI}O_2(phthalate)_3 \cdot 2H_2O$ (mean = 2.46 Å).[9b]

The Np−$C_c$ distances in $Np^{VI}O_2(AcO)^+$ and $Np^{VI}O_2(AcO)_3^-$ (2.87 Å) are identical and in agreement with bidentately coordinated acetate in crystal structures of $NaNp^{VI}O_2(AcO)_3$ (2.84 Å)[9a] and $NaU^{VI}O_2(AcO)_3$ (2.85 Å).[25] If carboxylate is bound to $Np^{VI}$ in monodentate coordination, the Np−$C_c$ distance is around 3.2−3.6 Å,[13a,26,27] because the Np−$O_{eq}$−$C_c$ angle is enlarged. The strong MS peak of $O_{ax}$−Np−$O_{ax}$ at twice the distance of Np−$O_{ax}$ may interfere with the scattering contribution of $C_c$ of monodentate acetate. However, no enhanced intensity was observed in the concerned spectral region. This agrees with the energetic point of view, where bidentate acetate coordination should be preferred because of the lower formation entropy due to the chelating effect.

The coordination number of $O_{eq}$ ($N_{eq}$) of $Np^{VI}O_2^{2+}$(aq) was 4.5 ± 0.3, in line with the coordination $Np^{VI}O_2(H_2O)_5^{2+}$. The shorter Np−$O_{eq}$ distance in $Np^{VI}O_2^{2+}$(aq) than that in $Np^{VI}O_2(AcO)_3^-$ may also be suggestive of $Np^{VI}O_2(H_2O)_5^{2+}$ with pentagonal-bipyramidal geometry.[3g] For $Np^{VI}O_2(AcO)^+$, $N_{eq}$ (= 4.7 ± 0.3) is also close to 5, and the number of coordinated acetates ($N_{AcO}$ = 1.2 ± 0.4) can be regarded as 1. As described above, the coordination of acetate is likely to be bidentate. Thus, we assume that $Np^{VI}$ in this species is surrounded by two $O_{eq}$ atoms from acetate and three $O_{eq}$ atoms from $H_2O$, i.e., $Np^{VI}O_2(AcO)(H_2O)_3^+$ in a pentagonal-bipyramidal coordination polyhedron. In comparison, $Np^{VI}O_2(AcO)_3^-$ shows $N_{eq} = 5.4 \pm 0.3$ and $N_{AcO} = 2.7 \pm 0.8$, corresponding to three bidentate acetate ligands. $Np^{VI}O_2(AcO)_3^-$ in solution should have the same hexagonal-bipyramidal structure as that in the solid sodium salt.[9a] In summary, the proposed structure of each $Np^{VI}O_2(AcO)_n^{2-n}$ ($n = 0$, 1, 3) is depicted in Scheme 1. As mentioned above, the structural parameters of $Np^{VI}O_2(AcO)_2$(aq) could not be determined because of the large noise in its EXAFS spectrum. However, it can be assumed that the neptunyl(VI) diacetate occurs as $Np^{VI}O_2(AcO)_2(H_2O)_2$ in accordance with $U^{VI}O_2(AcO)_2(H_2O)_2$ obtained from crystal structure analysis.[28]

**3.2. Stability Constants and Structures of Neptunyl(V) Acetate Complexes.** UV−vis−NIR absorption spectra of $Np^V$ ($2.78 \times 10^{-3}$ M) with 1.00 M AcOH at $I$ = 0.30 M $(H,NH_4)ClO_4$ and different pHs are shown in Figure 4. Full spectra are also displayed in Figure S6 in the Supporting Information. Each of them shows the absorption bands characteristic for f−f transitions of $Np^V$ in the $5f^2$ configuration.[15,16] With increasing pH, systematic spectral changes were observed, but again there were no isosbestic points. The absorbance around 430, 475, 590, and 630 nm increases from pH 0.57 to 3.13, while it decreases from pH 3.29 to 4.31. Furthermore, the absorption peaks around 630, 690, and 980 nm show red shifts with increasing pH from 3.71 to 4.31. These results are indicative of the presence of several complexation equilibria. Because hydrolysis of $Np^V$ is negligible up to pH 4.5,[2b,c] the observed pH dependence is assigned to the multistep complexation reactions of neptunyl(V) with acetate. The existence of the neptunyl(V) triacetate complex, $Np^VO_2(AcO)_3^{2-}$, isolated as the $Ba^{2+}$ salt[10a] is a strong indicator that the limiting species in the $Np^V$ series is also the 1:3 complex. Therefore, the following three-step complexation equilibria in aqueous solution can be expected:

$$Np^VO_2^+ + AcO^- = Np^VO_2(AcO)(aq) \quad (4)$$

$$Np^VO_2^+ + 2AcO^- = Np^VO_2(AcO)_2^- \quad (5)$$

$$Np^VO_2^+ + 3AcO^- = Np^VO_2(AcO)_3^{2-} \quad (6)$$

Even at the end of the pH series, the sample solution seems to be a mixture of $Np^VO_2(AcO)_n^{1-n}$ ($n = 0-3$), because the spectra show a progression until the last sample. The stability constants of neptunyl(V) acetate complexes were estimated by least-squares refinement of parameters describing the quantitative ratio of the UV−vis−NIR spectra shown in Figure 4. All three eqs 4−6 were necessary to fully reproduce the pH dependence of the UV−vis−NIR spectrum. The fits show that the limiting species occurs to only 49% even at the highest pH. Absorption spectra of the extracted individual

(24) (a) Alcock, N. W.; Esperås, S. *J. Chem. Soc., Dalton Trans.* **1977**, 893–896. (b) Fischer, A. *Z. Anorg. Allg. Chem.* **2003**, *629*, 1012–1016.
(25) (a) Zalkin, A.; Ruben, H.; Templeton, D. H. *Acta Crystallogr.* **1982**, *B38*, 610–612. (b) Templeton, D. H.; Zalkin, A.; Ruben, H.; Templeton, L. K. *Acta Crystallogr.* **1985**, *C41*, 1439–1441. (c) Navaza, A.; Charpin, P.; Vigner, D. *Acta Crystallogr.* **1991**, *C47*, 1842–1845.
(26) Mentzen, B. F. *Acta Crystallogr.* **1977**, *B33*, 2546–2549.
(27) Mentzen, B. F.; Puaux, J.-P.; Loiseleur, H. *Acta Crystallogr.* **1977**, *B33*, 1848–1851.
(28) Grigoriev, M. S.; Antipin, M. Y.; Krot, N. N. *Acta Crystallogr.* **2005**, *E61*, m2078–m2079.

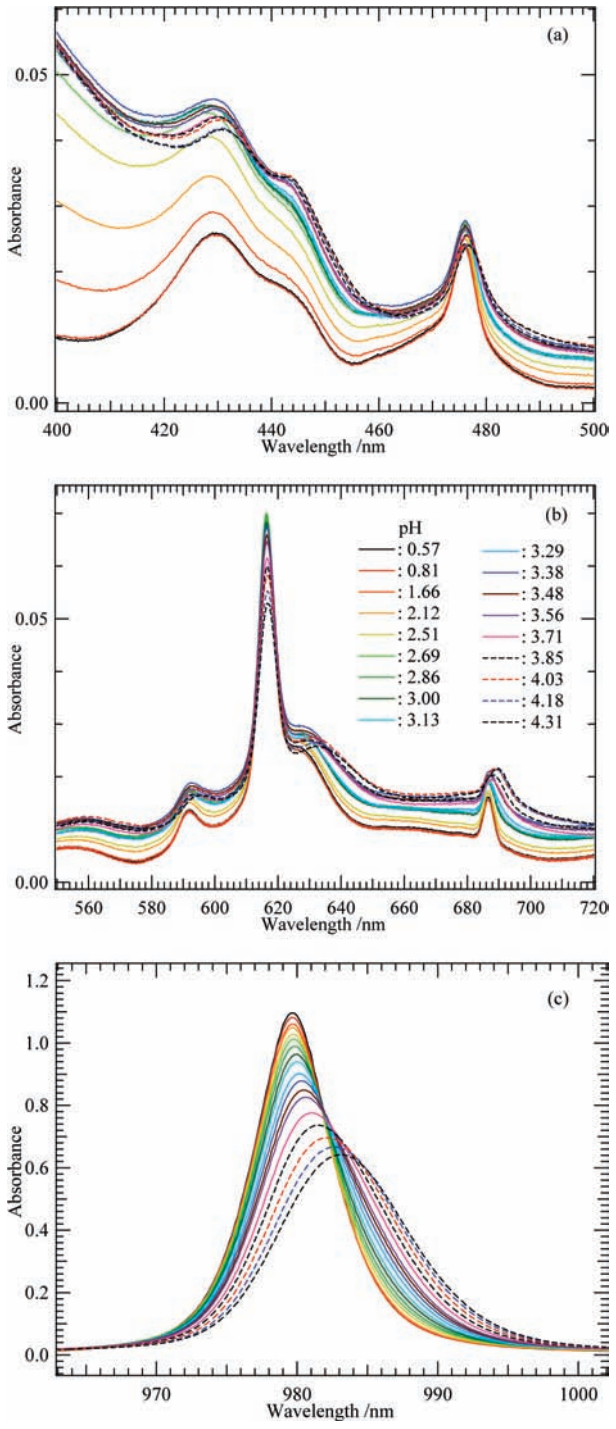


**Figure 4.** UV−vis−NIR absorption spectra of $Np^V$ ($2.78 \times 10^{-3}$ M) with 1.00 M AcOH at $I$ = 0.30 M $(H,NH_4)ClO_4$ and different pHs (0.57−4.31).

$Np^VO_2(AcO)_n^{1-n}$ ($n$ = 0−3) species are displayed in Figure S7 of the Supporting Information. The resulting stability constants of neptunyl(V) acetates are listed in Table 1. These stability constants were used to calculate the species distribution in a solution of 20 mM $Np^V$ with 1 M AcOH at $I$ = 0.3 M (Figure 5).

Np $L_{III}$-edge XAFS of $Np^V$ ($2.00 \times 10^{-2}$ M) with 1.00 M AcOH at $I$ = 0.30 M $(H,NH_4)ClO_4$ were recorded for four different pH values (0.60, 2.72, 3.69, and 4.27). The obtained $k^3$-weighted EXAFS (Figure 6) show systematic

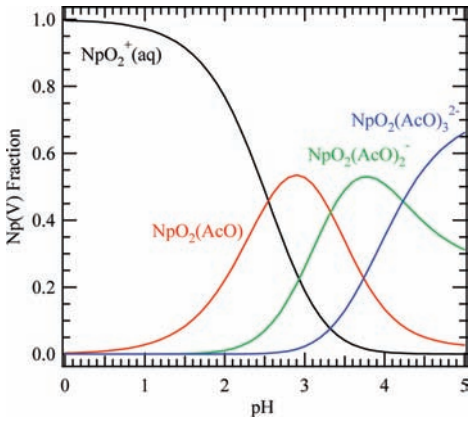


**Figure 5.** Species distribution of neptunyl(V) acetates derived from UV−vis−NIR spectroscopy at 0.02 M $Np^V$ and 1 M AcOH in $I$ = 0.3 M.

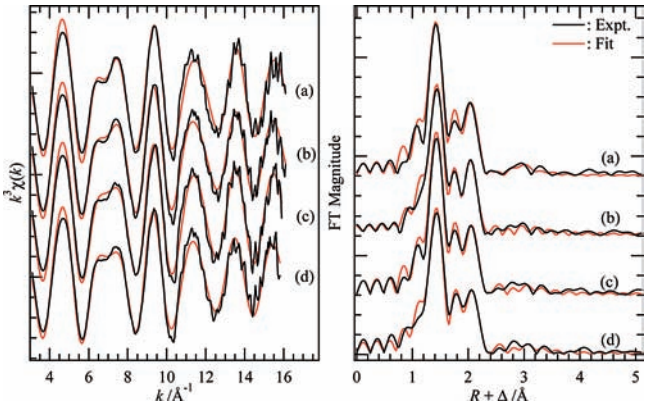


**Figure 6.** $k^3$-weighted Np $L_{III}$-edge EXAFS spectra (left) and their FTs (right) of the neptunyl(V) acetate series at pH 0.60 (a), 2.72 (b), 3.69 (c), and 4.27 (d).

variations around 6−8 Å$^{-1}$, indicating a structural modification around neptunyl(V) due to complexation with acetate. The changes are small but observable more clearly in their superposition (Figure S8 of the Supporting Information). In the XANES region of Figure S8 of the Supporting Information, the spectral change due to the complexation of $Np^V$ is also detectable.

To obtain the structural information of the neptunyl(V) acetate complexes in solution, curve fits using the FTs of the $k^3$-weighted EXAFS spectra (Figure 6, right) were performed. The resulting structural parameters at different pHs are listed in Table 3. Note that the parameters in this table correspond to statistically weighted averages of species because the sample solutions comprise mixtures of different neptunyl(V) acetate complexes. In the FTs of Figure 6, the intense peak at around $R+\Delta$ = 1.42 Å is attributable to the $O_{ax}$ shell of $Np^V$. The Np−$O_{ax}$ distances at different pHs are in the range of 1.83−1.85 Å, which is in agreement with other $Np^V$ species in both solids and solutions.[3g,10] The Np−$O_{eq}$ shell of the coordinated $H_2O$ and/or acetate resulted in a peak around $R+\Delta$ = 2.1 Å. The Np−$O_{eq}$ distance remains unchanged at 2.51 Å for the complete series. Furthermore, the $O_{eq}$ shell was fit with only one distance, indicating that oxygen atoms from $H_2O$ and acetate cannot be distinguished considering the distal resolution $\Delta R$ of 0.12 Å [$\Delta R = \pi/2\Delta k$, for a $k$-range window ($\Delta k$) of 12.9 Å$^{-1}$]. The

**Table 3.** Structural Parameters from EXAFS Curve Fits for the $Np^V$ Series with AcOH at Different pHs[a]

| | pH 0.60 ($\Delta E_0$ = 4.5 eV) | | | pH 2.72 ($\Delta E_0$ = 8.2 eV) | | |
|---|---|---|---|---|---|---|
| shell | $N$ | $R$/Å | $\sigma^2$/Å$^2$ | $N$ | $R$/Å | $\sigma^2$/Å$^2$ |
| $O_{ax}$ | 2 [b] | 1.83 | 0.0013 | 2 [b] | 1.84 | 0.0013 |
| $O_{eq}$ | 4.5 | 2.51 | 0.0063 | 4.5 | 2.51 | 0.0061 |
| $C_c$ | | | | 0.7 | 2.91 | 0.0095 |
| $O_{ax}$ (MS) | 2 [b] | 3.63 | 0.0025 | 2 [b] | 3.68 | 0.0063 |
| | pH 3.69 ($\Delta E_0$ = 8.3 eV) | | | pH 4.27 ($\Delta E_0$ = 8.5 eV) | | |
| shell | $N$ | $R$/Å | $\sigma^2$/Å$^2$ | $N$ | $R$/Å | $\sigma^2$/Å$^2$ |
| $O_{ax}$ | 2 [b] | 1.84 | 0.0009 | 2 [b] | 1.85 | 0.0014 |
| $O_{eq}$ | 5.2 | 2.51 | 0.0074 | 5.1 | 2.51 | 0.0077 |
| $C_c$ | 1.9 | 2.90 | 0.0098 | 2.5 | 2.93 | 0.0103 |
| $O_{ax}$ (MS) | 2 [b] | 3.68 | 0.0054 | 2 [b] | 3.68 | 0.0038 |

[a] $\sigma^2$ = Debye−Waller factor. [b] Fixed parameter.

$Np-O_{eq}$ distance of 2.51 Å is slightly shorter than that in the solid $BaNp^VO_2(AcO)_3$ (2.560, 2.556, and 2.516 Å).[10a] In this solid structure, the oxygen atoms of the coordinated acetate are shared between neptunium and barium. Such an interaction may result in an elongation of the $Np-O_{eq}$ distance. This should not be the case in solution, however, because the neptunyl(V) acetate species have no or only a small negative charge (1− and 2−) and hardly interact with counterions in solution.

Bidentate acetate coordination should give rise to a SS peak of the $Np-C_c$ shell as described above. However, this $C_c$ peak is discernible neither in FT magnitude (Figure 6, right) nor in FT imaginary parts (Figure S9 of the Supporting Information). In order to extract this hidden contribution, we subtracted the spectra at pH 2.72, 3.69, and 4.27 from that at pH 0.60. Although the resulting difference spectra (Figure S10 of the Supporting Information) are accompanied by considerable noise, an oscillation can be observed in the $k$ range of 3.1−6.1 Å$^{-1}$. Because the structural parameters of the $Np-O_{ax}$ and $Np-O_{eq}$ shells are almost constant among all samples, as shown in Table 3, the EXAFS oscillation observed in Figure S10b of the Supporting Information is attributable mainly to the $Np-C_c$ shell. The oscillation at pH 4.27 is most resolved and can be represented by the $Np-C_c$ shell with $R$ = 2.93 Å. From the curve-fit result for each original EXAFS spectrum, the $Np-C_c$ distances were determined as 2.91−2.93 Å (Table 3), which are slightly longer than those in neptunyl(VI) acetates (2.87 Å; Table 2) and also comparable with those of the bidentate acetate and carbonate in solid $BaNp^VO_2(AcO)_3$ ($Np-C_c$=2.92 Å),[10a] $Np^VO_2(AcO)(imidazole)_2(H_2O)$ ($Np-C_c$=2.91 Å),[10c] and $U^VO_2(CO_3)_3^{5-}$ ($U-C_c$ = 2.93 Å).[3c,e] No remarkable peaks attributable to the $Np-C_t$ shell around 4.4 Å were detected in Figure 6 (cf. 4.38 Å in $Np^{VI}O_2(AcO)_3^-$; Table 2).

**3.3. Electrochemistry of $Np^{V/VI}$ with Acetic Acid.** If all equilibria in a system of interest and their equilibrium constants are properly known, the correlation between the stability range of the predominant species as a function of the pH and electrochemical potential ($E$) of two corresponding redox species can be figured out in a Pourbaix diagram. For this correlation, we use the stability constants of the neptunyl(VI) and -(V) acetate complexes summarized in Table 1. The $Np^{V/VI}$ redox potential (eq 7) and the protonation constant of acetate (eq 8) were taken from the literature.[2b,c,19]

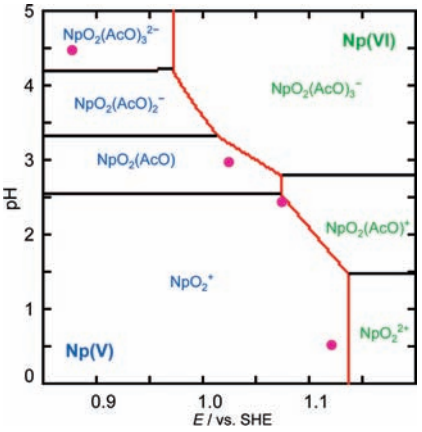


**Figure 7.** Pourbaix diagram of $Np^{V/VI}$ (total Np concentration: 5 mM) with 1 M AcOH at $I$ = 0.3 M. Red line: boundary between $Np^V$ and $Np^{VI}$ ($E°_{V/VI}$). Purple dot: formal potential ($E°'$) from CVs of Figure 8.

$$Np^{VI}O_2^{2+} + e^- = Np^VO_2^+ \quad \log K_{V/VI} = 19.19 \quad (7)$$

$$E°_{V/VI} = 1.135 \text{ V vs SHE}$$

$$H^+ + AcO^- = AcOH \quad \log K_{AcO} = 4.45 \quad (8)$$

where SHE is the standard hydrogen electrode. These constants were estimated by an ionic strength correction at $I$ = 0.3 M using the specific ion interaction theory.[2c] Because $\log K_{AcO}$ in eq 8 is consistent with that experimentally derived ($\log K_{AcO}$ = 4.51 at $I$ = 0.30 M),[29] the ionic strength correction has been done successfully. On the basis of the equilibrium constants of eqs 1−8,[30] the Pourbaix diagram of the $Np^{V/VI}$ redox couple (total neptunium concentration: 5 mM) with 1 M AcOH at $I$ = 0.3 M is calculated and displayed in Figure 7. In this figure, the red line is the boundary between the $Np^V$ and $Np^{VI}$ species; i.e., it represents the pH dependence of the $Np^{V/VI}$ redox potential, $E°_{V/VI}$.

To examine the validity of Figure 7, we measured CVs of $Np^{VI}$ ($5.0 \times 10^{-3}$ M) with 1.00 M AcOH in $I$ = 0.30 M $(H,NH_4)ClO_4$ at pH 0.53, 2.46, 2.99, and 4.45. The CVs are shown in Figure 8. The observed peak potentials and related data are summarized in Table S1 of the Supporting Information. At pH 0.53 (Figure 8a), where the coordination of acetate is not significant, a couple of cathodic and anodic peaks of $Np^{V/VI}$ were observed at 0.912 V vs Ag/AgCl as a formal potential $E°'$. At pH 2.46, 2.99, and 4.45, the sample solutions should be a mixture of $Np^{VI}O_2(AcO)_n^{2-n}$ (as oxidants) and $Np^VO_2(AcO)_n^{1-n}$ (as reductants). Nevertheless, only one redox couple of $Np^{V/VI}$ was observed in Figure 8b−d. This implies that the kinetics of the complex formation equilibria of

(29) Chen, J.-F.; Xia, Y.-X.; Choppin, G. R. *Anal. Chem.* **1996**, *68*, 3973–3978.

(30) In this calculation, the stability constants of the neptunyl(VI) acetate complexes ($n$ = 1−3) from UV−vis−NIR absorption spectroscopy were taken.

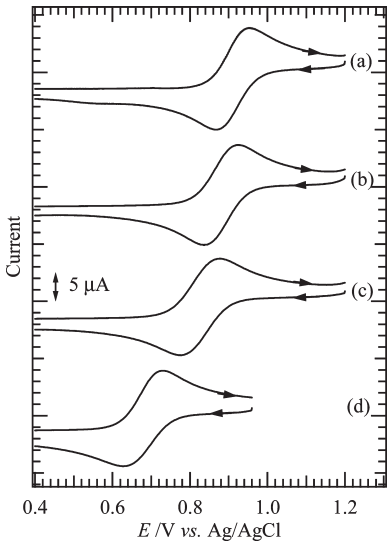


**Figure 8.** CVs of $Np^{VI}$ ($5.0 \times 10^{-3}$ M) with 1.00 M AcOH at $I$ = 0.30 M $(H,NH_4)ClO_4$ and pH 0.53 (a), 2.46 (b), 2.99 (c), and 4.45 (d) on a platinum disk working electrode. Scan rate: 10 mV $s^{-1}$. Initial scan direction: cathodic.

neptunyl(VI) and -(V) acetates follows the potential sweep in the CV experiment (scan rate: 10 mV $s^{-1}$).

With increasing pH, the observed $E^{\circ\prime}$ shifts to negative potentials. This arises from the complexation of neptunyl(VI) and -(V) with acetate and should follow the curve as predicted in Figure 7. The formal potential $E^{\circ\prime}$ of $Np^{V/VI}$ at each pH is plotted as a function of the pH in Figure 7 as purple dots. The potential difference between Ag/AgCl and SHE reference electrodes has been taken into account [0 V vs SHE = +0.196 V vs Ag/AgCl (3 M NaCl)].[31] As a result, the pH dependence of the predicted $E^{\circ}_{V/VI}$ is comparable with that of $E^{\circ\prime}$ obtained experimentally. It should be emphasized that the Pourbaix diagram relies only on thermodynamic information and does not take any kinetic parameters from complexation and electron transfer into account. On the other hand, the CV is affected by both thermodynamics and kinetics, and it is, furthermore, sensitive to diffusion of a substance onto the electrode surface. Therefore, the difference between the predicted $E^{\circ}_{V/VI}$ and the experimental $E^{\circ\prime}$ could not be discussed quantitatively. Nevertheless, $E^{\circ}_{V/VI}$ seems to be in qualitative agreement with $E^{\circ\prime}$, indicating the validity of the assumed complexation reaction schemes of neptunyl(VI) and -(V) with acetate (eqs 1−6).

(31) Du, R.-G.; Hu, R.-G.; Huang, R.-S.; Lin, C.-J. *Anal. Chem.* **2006**, *78*, 3179–3185.

## 4. Conclusion

In this study, we have investigated the stability and structure of neptunyl(VI) and -(V) acetate complexes in aqueous solution by combining UV−vis−NIR and XAFS spectroscopy. In the neptunyl(VI) acetate system, the formation constants of $Np^{VI}O_2(AcO)^+$, $Np^{VI}O_2(AcO)_2(aq)$, and $Np^{VI}O_2(AcO)_3^-$ were independently determined from UV−vis−NIR and XAFS titration experiments. The extracted XAFS spectra of $Np^{VI}O_2^{2+}(aq)$, $Np^{VI}O_2(AcO)^+$, and $Np^{VI}O_2(AcO)_3^-$ provided coordination of the species, summarized in Scheme 1. In the neptunyl(V) acetate system, it was suggested that neptunyl(V) forms complexes with acetate in three steps, similar to neptunyl(VI) acetates. The stability constants of $Np^{V}O_2(AcO)(aq)$, $Np^{V}O_2(AcO)_2^-$, and $Np^{V}O_2(AcO)_3^{2-}$ were determined here only by the UV−vis−NIR titration. The present result is corroborated by the structural information from XAFS and the electrochemical behavior of $Np^{V/VI}$ in the presence of AcOH at various pHs. This study has demonstrated that XAFS is a useful tool in providing structural data as helpful information to determine the proper reaction scheme.

**Acknowledgment.** We thank Dr. Atsushi Ikeda-Ohno (JAEA) for helpful advice. S.T. was supported by a stipend from the Alexander von Humboldt Foundation. This work was supported by the Deutsche Forschungsgemeinschaft under Contract HE 2297/2-2.

**Supporting Information Available:** UV−vis−NIR absorption spectra of $Np^{VI}$ with AcOH at different pHs, UV−vis−NIR absorption spectra of individual $Np^{VI}O_2(AcO)_n^{2-n}$ complexes, XAFS spectra of $Np^{VI}$ with AcOH at different pHs, FTs of $k^3$-weighted EXAFS spectra of $Np^{VI}$ with AcOH at different pHs, XANES and $k^3$-weighted EXAFS spectra of individual $Np^{VI}O_2(AcO)_n^{2-n}$ complexes, UV−vis−NIR absorption spectra of $Np^{V}$ with AcOH at different pHs, UV−vis−NIR absorption spectra of individual $Np^{V}O_2(AcO)_n^{1-n}$ complexes, XANES and $k^3$-weighted EXAFS spectra of $Np^{V}$ with AcOH at different pHs, FT imaginary parts of $k^3$-weighted EXAFS spectra of $Np^{V}$ with AcOH at different pHs, different $k^3$-weighted EXAFS spectra of $Np^{V}$ with AcOH, and a table of peak and formal potentials of a $Np^{V/VI}$ redox couple with AcOH in Figure 8. This material is available free of charge via the Internet at http://pubs.acs.org.